

#### Contents lists available at ScienceDirect

# Polymer

journal homepage: www.elsevier.com/locate/polymer





# Synthesis and thermomechanical characteristics of zwitterionic poly (arylene ether sulfone) copolymers

Yi Yang <sup>a, 1</sup>, Hoda Shokrollahzadeh Behbahani <sup>a</sup>, Brian F. Morgan <sup>b</sup>, Frederick L. Beyer <sup>b</sup>, Alexis Hocken <sup>a, 2</sup>, Matthew D. Green <sup>a, \*</sup>

#### ARTICLE INFO

#### Keywords: Sulfobetaine zwitterion Poly(arylene ether sulfone)s Polyelectrolyte Random copolymer

#### ABSTRACT

Charge-containing polymeric materials have been widely studied for a range of applications. The fundamental relationships between the charge species, charge density, and the microscale morphology of charge-containing polymers are critical for defining the application in which they may be used. In this work, a series of thermoplastic poly(arylene ether sulfone) (PAES) copolymers with controllable sulfobetaine charge contents (0–100 mol %) and high molecular weights (Mw  $\sim$  65 kDa) were prepared. All the zwitterionic PAESs synthesized showed thermal stability up to 250 °C. DSC and tensile tests showed a decreased  $T_g$  and mechanical strength with the incorporation of increasing charge density, which suggests a plasticization effect by the charged group. Electron microscopy and X-ray scattering data confirmed the absence of microphase separation in the ion-containing random copolymer system, which corroborated with the observation of a single  $T_g$  for all zwitterionic copolymers studied. Furthermore, the relative hydrophilicity of the samples was evaluated by water uptake measurements, which revealed that the water uptake of the zwitterionic PAESs can reach up to 64% for the 72 mol% zwitterion copolymer while the free-standing film in the wet state still maintains a Young's modulus of 185 MPa. The thermoplastic charge-containing copolymers in this work demonstrated potential for applications such as coatings or water purification membranes, in which balancing hydrophilicity, processibility, and thermomechanical performance are important.

#### 1. Introduction

Charged polymers have been widely used in a range of applications, especially water purification membranes. However, there is a tradeoff relationship in water purification between the permeability and water/ion permeability selectivity of the desalination membranes. Zwitterions are charged molecules that contain a covalently bonded cation and anion and are potential candidate materials for membranes. The unique structure of zwitterions offers an extremely high polarity and hydration capability [1,2]. Additionally, zwitterions improve fouling resistance on membrane surfaces due to their high intrinsic hydrophilicity, which was proposed to form a protective hydration layer via strong electrostatic interaction between zwitterions and water molecules [3–6].

In order to limit the swelling induced by the highly hydrophilic

zwitterionic groups, a rigid backbone, i.e., poly(arylene ether sulfone)s (PAES), is utilized in this work to restrict the membrane from swelling and maintain the overall perm-selectivity and mechanical strength. In parallel, high mechanical strength of the membrane is crucial to withstand the high pressures applied during seawater desalination; thus, a sufficiently high molecular weight PAES is needed for optimal and well-controlled membrane performance and mechanical integrity. A variety of PAES-based amphiphilic polyelectrolytes have been synthesized by surface grafting pendant zwitterionic side chains onto PAES substrates [3,7–11] as well as by preparing block copolymers containing PAES and other sulfobetaine-containing segments [10,12,13]. However, very few studies have been done on random copolymerization of amphiphilic PAES, which comparatively induces less chance for intermolecular interactions among the zwitterionic segments and will be discussed further

a Department of Chemical Engineering, School for Engineering of Matter, Transport and Energy, Arizona State University, Tempe, AZ, 85287, USA

<sup>&</sup>lt;sup>b</sup> U.S. Army Research Laboratory, Aberdeen Proving Ground, MD, 21005, USA

<sup>\*</sup> Corresponding author.

E-mail address: mdgreen8@asu.edu (M.D. Green).

<sup>&</sup>lt;sup>1</sup> Present address: Assembly & Test Technology Development, Intel corporation, Chandler, AZ 85226, USA.

<sup>&</sup>lt;sup>2</sup> Present address: Department of Chemical Engineering, Massachusetts Institute of Technology, 77 Massachusetts Avenue, Cambridge, Massachusetts 02139, United States.

through this work. Zhang and coworkers [14,15] prepared cardo sulfobetaine poly(arylene ether sulfone) (PES-SB) random copolymer membrane and showed a decrease in water contact angle after the incorporation of the sulfobetaine group, while the hydrophilicity improvement was still limited due to the strong inter- and/or intramolecular interaction between the ammonium group and sulfonate group and the moderate ion exchange capacity (IEC ~ 1 mmol/g). Increasing the IEC will often lead to an increase in water uptake due to the addition of hydrophilicity and hydration of charged sites. The swelling from water can have adverse effects on the hydrated membrane mechanical properties. A large water uptake may also lead to a decrease in the concentration of fixed charge groups. A high fixed charge concentration is preferred for desalination membrane applications as it is correlated with a higher Donnan potential which leads to better salt rejection for RO membranes and decreased transport of co-ions for electrodialysis membranes [16-19]. It is necessary and urgent, therefore, to improve IEC limits whilst maintaining a high fixed charge group concentration and suitable mechanical properties to control the charge content precisely via novel structure designs.

In the present work, we report on the synthesis and properties of a series of sulfobetaine-based zwitterionic PAES random copolymers. Ultimately, we determined and utilized the optimal conditions to prepare a series of high molecular weight zwitterionic PAES random copolymers (full details in Fig. S1). The effects of charge content on the  $T_{\rm g}$ , thermal stability, mechanical properties, IEC, water uptake, and morphology are discussed. The potential of the presented novel zwitterionic PAES copolymers is emphasized by efficient and controllable synthesis route for mechanically strong films, which will be examined for membrane separations in the future.

#### 2. Experimental section

## 2.1. Reagents

4,4'-Difluorodiphenyl sulfone (DFDPS, > 98%) was purchased from Thermo Fisher Scientific Chemical and recrystallized from diethyl ether before use. Bisphenol A (BPA, > 99%) was purchased from BDH® VMR analytical and recrystallized from acetic acid/water (1:1 v/v) before use. 2,2'-Diallylbisphenol A (DABA, 85%) was purchased from Sigma-Aldrich and purified by distilling impurities out of DABA in the presence of tetrahydrofuran (THF) under vacuum before use. THF and toluene (99.8%) were purchased from Sigma-Aldrich and used after passing through M. Braun SPS-800 solvent purification system. Dimethylsulfoxide (DMSO, anhydrous, ≥ 99.9%), Dimethylformamide (DMF, ≥ 99.8%), 1,3-propanesultone (1,3-PS), 2-(dimethylamino)ethanethiol, and 2,2-dimethoxy-2-phenylacetophenone (DMPA, 99%) were purchased from Sigma-Aldrich and used as received. Potassium carbonate (K<sub>2</sub>CO<sub>3</sub>, ≥98%) was purchased from Sigma-Aldrich and vacuum dried overnight before use. Deuterated chloroform (CDCl<sub>3</sub>, 99.8 atom% D, 0.03% (v/v) TMS) was purchased from BDH® VMR analytical and used as received.

#### 2.2. Instrumentation

 $^{1}$ H NMR spectroscopy was performed on a Varian 400 MHz spectrometer using deuterated chloroform (CDCl<sub>3</sub>) to determine the copolymer chemical structures. Samples were prepared as 20 mg of dried polymer dissolved in deuterated chloroform. Chemical shifts are given in ppm downfield from tetramethylsilane (TMS).

Size exclusion chromatography (SEC) was performed using a Waters Alliance e2695 HPLC system interfaced to a light scattering detector (miniDAWN TREOS) and an Optilab T-rEX differential refractive index (dRI) detector. The mobile phase was THF Optima (inhibitor-free) at a flow rate of 1.0 mL min<sup>-1</sup>, and samples were calibrated against Pressure Chemical Company low dispersity polystyrene standards of 30 kDa and 200 kDa using Astra v6.1 software. Sonicated and filtered solutions at a

concentration of  $\sim$ 1.0 mg mL $^{-1}$  polymer in THF were prepared for SEC.

Thermogravimetric analysis (TGA) was performed using a TA instruments TGA 2950. Measurements were carried out under nitrogen at a heating rate of 10  $^{\circ}\text{C/min}.$ 

Differential scanning calorimetry (DSC) was performed using a Q2000 from TA Instruments. Samples of  $\sim\!\!5$  mg were placed in crimped aluminum pans and heated to 200 °C, cooled to -50 °C, and then heated to 300 °C. The heating and cooling rate were set to 5 °C/min and 10 °C/min, respectively. The reported values of  $T_gs$  were taken from the second heating scan.

Wide-angle X-ray scattering (WAXS) experiments in transmission mode were performed on films ranging in thickness from 130 to 450  $\mu m$  on a Bruker AXS LLC D8 ADVANCE diffractometer with a Cu source ( $\lambda=1.542$  Å). Data were collected with a Bruker VÅNTEC two-dimensional (2D) area detector. All data corrections and analysis were performed using Wavemetrics Igor Pro and procedures available from Argonne National Laboratory [20,21].

Scanning transmission electron microscope (STEM) in TEM mode was performed using the FEI Titan 80–300 aberration corrected probe operated at 300 keV. All copolymer films were submerged in a 2% aqueous copper (II) chloride (CuCl $_2$ ) solution for 4 h to stain the sulfobetaine groups to enhance the imaging contrast. The stained films were embedded in Embed 812 epoxy resin overnight. Ultrathin ( $\sim$ 40 nm) sections were obtained by using an ultramicrotome and were placed on copper grids (G200, Ted Pella®).

An Instron 5943 equipped with submersible pneumatic grips and a water bath was used to perform uniaxial tensile testing of the dense membranes. ASTM D-1708 was used to cut samples into dog bone geometry; the samples were then extended at a rate of 1 mm/min at room temperature until breakage. Replicates were analyzed, and the average values are reported.

To measure the water uptake, the membranes were dried using a Fisherbrand Isotemp Model 281A Vacuum Oven for 24 h at room temperature. Then, the samples were submerged and left to sit in deionized water at room temperature for 24 h. The samples were then taken out, blotted dry to remove surface droplets and weighed with a Classic MS Series Mettler Toledo scale. The water uptake is measured using the equation below.

Water uptake (%) = 
$$\left(\frac{w_w - w_d}{w_d}\right) \times 100$$

Here,  $w_w$  and  $w_d$  are the weights of the wet and dry sample, respectively. Replicates were analyzed and the average water uptake content was reported.

The fixed charge concentration of membranes,  $C_x^m$ , is calculated using the equation below.

$$C_x^m = \frac{IEC \times \rho_w}{WU}$$

In the above equation, IEC, which is the quantity of charged groups on the polymer backbone per weight of dry polymer is measured from the molecular weight of the repeating unit of polymers (mmol/g), WU is the water uptake (g water/g of dry polymer) and  $\rho_w$  is the density of water, assumed to be 1.0 g/mL.

# 2.3. Synthesis of allyl-modified poly(arylene ether sulfone) (A-PAES) copolymers

The allyl-containing poly(arylene ether sulfone) copolymer was synthesized via conventional polycondensation of poly(arylene ether sulfone)s [13] with modified reaction conditions. The series of A-PAES copolymers were synthesized in the same fashion with an off-set stoichiometry of r=0.94 between phenol group and aryl halide group, except with different BPA/DABA ratios for corresponding targeted functionality contents in the synthesized polymer structure (i.e., for

Y. Yang et al. Polymer 264 (2023) 125522

Scheme 1. Synthesis route to prepare zwitterionic PAES-co-SBAES-XX (XX = mole fraction of zwitterionic units, and ranges from 0-100%).

A-PAES-22, the feed molar ratio among DFDPS, BPA and DABA monomers was 100:70.5:23.5, while the actual A-PAES repeat unit content is 22% from NMR results, which will be discussed in result section). Take A-PAES-72 as an example herein. BPA (0.792 g, 3.476 mmol), DABA (3.212 g, 10.428 mmol), DFDPS (3.757 g, 14.791 mmol), and  $K_2CO_3$ (2.015 g, 14.599 mmol) were added to a three-neck, 250-mL flask equipped with a condenser, Dean Stark trap, nitrogen inlet/outlet, and a mechanical stirrer. DMSO (50 mL) and toluene (15 mL) were added to the flask to dissolve the monomers. The solution was heated under reflux at 135 °C for ~3 h while the toluene-water azeotrope and toluene residue was completely removed from the reaction mixture. The reaction was continued under static nitrogen atmosphere for another 1-4 h at 135 °C. The reaction mixture was cooled to room temperature and diluted with 200 mL of THF. It was filtered to remove the salt and precipitated by addition to stirring DI water. The polymer was filtered and dried under vacuum at 100 °C for 24 h. Then, the polymer was dissolved in THF, passed through a 0.45  $\mu m$  Teflon® filter, then isolated by precipitation in DI water. The product (A-PAES-72) was freeze-dried at -89 °C under vacuum for 24 h.

It should be noted that different reaction solution concentrations were tested during the A-PAES copolymer synthesis. The monomer concentration in the DMSO/toluene solvent mixture after the toluene-water azeotrope was completely removed from the reaction mixture (within the first 3 h of the reaction) was 0.47, 0.52, or 0.64 mmol/L. The optimal reaction solution concentration was then selected for the rest of the series of A-PAES polymerization.

## 2.4. Synthesis of tertiary amine-modified PAES (TA-PAES) copolymers

The synthesized A-PAES-72 copolymer (5 g, 14.805 mmol of allyl group), 2-(dimethylamino)ethanethiol (20.975 g, 10 eq), and DMPA (1.134 g, 0.3 eq) were dissolved in DMF (100 mL) to perform a post-polymerization modification via the thiol-ene click reaction. The reactor flask was purged with nitrogen for 15 min. Irradiation with UVGL-15 compact UV lamp (365 nm) was carried out for 2 h at 23 °C. The solution was concentrated using a rotary evaporator, and the polymer was then isolated by precipitation in DI water, and the product was freeze-dried at  $-89\ ^{\circ}\text{C}$  under vacuum for 24 h.

#### 2.5. Synthesis of PAES-co-SBAES copolymers

To a solution of TA-PAES-72 (5 g, 11.346 mmol of TA group) in DMF (100 mL), 1,3-propanesultone (2.772 g, 2 eq) was added. The solution was stirred at room temperature for 1 h and at 60 °C for 12 h. The solution was concentrated using a rotary evaporator, and the remaining solution was diluted with DMF (5 mL) and dialyzed against DMF in a dialysis tube (1 kDa MWCO) for 3 days. The DMF outside the dialysis tube was exchanged with fresh DMF every 2 h over the first 10 h and then every 6 h until completion. The polymer was then isolated by precipitation in DI water, and the product was freeze-dried at  $-89\ ^{\circ}\text{C}$  under vacuum for 24 h.

# 2.6. Film preparation

A 2.5 wt% solution of the polymer (in powder form) in DMF was prepared to make dense membranes. The solution was put in a sonication bath and stirred for 1 h until a homogeneous solution was formed. The solution was then passed through a 0.45  $\mu m$  PTFE filter and poured inside a Pyrex® flat-bottomed petri dish and left to sit at room temperature overnight. A non-hermetically sealed glass lid was put on top of the petri dish to degas the solution by equilibrating with the air above. To evaporate the solvent, the petri dish was put inside a vacuum oven set to temperatures of 22 °C, 40 °C and 80 °C, each for 24 h. The membrane was peeled off of the petri dish by addition of DI water. The membranes were stored in DI water.

#### 3. Results and discussion

The A-PAES copolymers (Scheme 1) were synthesized via polycondensation reactions [22–24] between 4,4'-difluorodiphenyl sulfone (DFDPS) and varying ratios of bisphenol A (BPA) and 2,2'-diallylbisphenol A (DABA). BPA (the non-allyl-containing monomer) and DABA (the allyl-containing monomer) represent the monomers that ultimately define the charge content in the copolymer. An off-set stoichiometry of the aryl halide relative to the phenol was used (1:0.94 halide:phenol) based on past experience [25] to optimize the molecular weight and obtain complete conversion. A series of the A-PAES copolymers with various allyl contents (0 mol%, 22 mol%, 45 mol%, 72 mol%, and 100

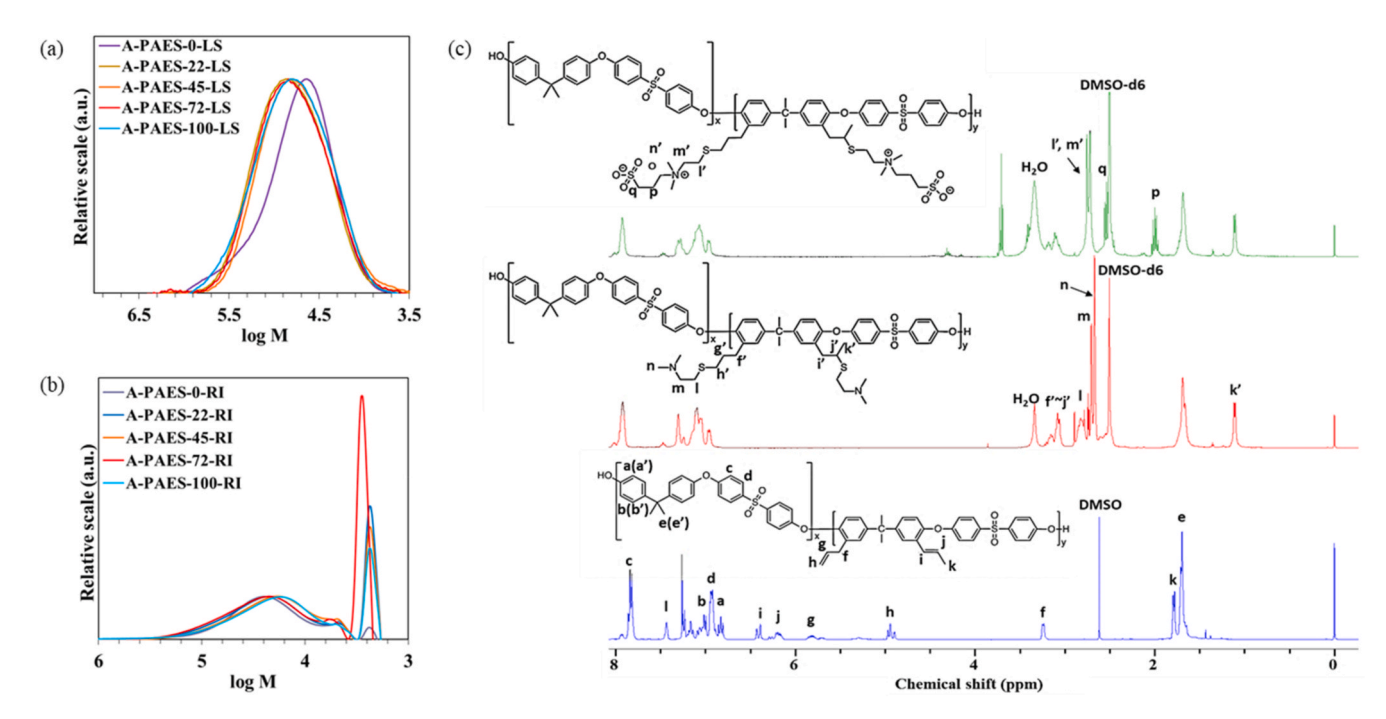


Fig. 1. SEC detector signals from the (a) light scattering (LS) detector and (b) refractive index (RI) detector is shown for A-PAES-XX. (c) <sup>1</sup>H NMR spectra of A-PAES copolymers (bottom), tertiary amine-modified PAES (TA-PAES) copolymers (middle), and zwitterionic PAES-co-SBAES copolymers (top), respectively. The spectra shown are representative spectra for the PAES-co-SBAES with an SBAES content of 72 mol%. The corresponding spectra for the other SBAES mole fractions are shown in Fig. S1c.

Table 1
The calculated allyl-containing repeat unit (A-PAES) contents (feed versus concentration determined using NMR spectroscopy, accounting of isomer content) and molecular weight and dispersity (from SEC).

Feed ratio (DABA:BPA)	A-PAES content (%)	Mn <sup>a</sup> (kDa)	Mw <sup>b</sup> (kDa)	Ð
0:100	0	34.9	64.7	1.84
25:75	22	32.9	62.4	1.90
50:50	45	33.2	62.5	1.88
75:25	72	34.3	63.7	1.86
100:0	100	33.3	65.0	1.95
50:50 75:25	45 72	33.2 34.3	62.5 63.7	1.88 1.86

<sup>&</sup>lt;sup>a</sup> Determined by SEC RI detector measurement.

mol%, namely A-PAES-XX, where XX indicates the molar fraction of allyl-containing repeat units) were synthesized using the monomer concentration determined above. The copolymers were analyzed by SEC (Fig. 1a and b) to determine the number-average and weight-average molecular weight and the  $\it D$ . The A-PAES copolymers had a consistent number-average molecular weight ( $M_n$ ) of  $33.7\pm0.7~kg~mol^{-1}$ , weight average molecular weight ( $M_w$ ) of  $63.7\pm1.1~kg~mol^{-1}$ , and  $\it D$  of  $1.89\pm0.03$ . The consistency highlights the ideal nature of the step-growth reactions and the ability to achieve high molecular weight and full conversion over the entire composition range.

Upon the incorporation of DABA in the copolymer, the peaks arising from the protons on –CH $_2$ CH=CH $_2$  appeared at 3.2, 5.8, and 4.9 ppm, (signal f, g, and h, respectively). Some thermal rearrangement to form the regioisomer occurred [26], and the isomerized form –CH=CHCH $_3$  showed up at 6.4, 6.2, and 1.8 ppm, (signal i, j, and k, respectively). Together, the presence of these peaks and the integrations indicate the successful incorporation of allyl-containing repeating units into the backbone. It is worth mentioning that the isomerization of the allyl group did not affect the reactivity during the post-polymerization functionalization reaction using the protocols herein. The A-PAES chemical structure depicted in Scheme 1 and Fig. 1c, where allyl and isomerized allyl groups are attached to the same repeat unit, is only for

illustration: it is also possible that two allyl groups or two isomerized allyl moieties are attached to the same repeat unit in the actual polymer structure. The integral of the peaks labeled  $f\sim k$ , when compared to the integral of the peak from the diphenyl sulfone (i.e., signal c), was used to determine the content of pendant allyl group covalently bonded to the PAES backbone. The integral ratio between peak  $f\sim h$  and  $i\sim k$  was quite useful to assess the extent of isomerization. The calculated allyl-containing repeat unit contents are compiled in Table 1 and are consistently below the feed ratios of 0, 25, 50, 75, and 100 mol%. This indicates that the synthesis strategy was successful, but that the reactivity of DABA versus BPA with DFDPS was slightly lower potentially due to steric effects.

A series of zwitterionic PAES-co-SBAES copolymers were synthesized by a two-step post-polymerization modification of A-PAES copolymers. First, the allyl moieties of the A-PAES copolymers were functionalized with 2-(dimethylamino)ethanethiol using a thiol-ene "click" reaction to obtain tertiary amine groups pendant to the polymer backbone. Next, a ring-opening reaction of 1,3-propanesultone was utilized to incorporate the sulfonate group and form the sulfobetaine functionality (Scheme 1). After the thiol-ene "click" reaction, peaks from the allyl group and its isomer (signal  $f \sim k$  in Fig. 1c) disappeared and new peaks showed up at 1.1 ppm and 2.67–3.2 ppm, which were attributed to the new tertiary amine moiety (signal l-n in Fig. 1c). The complete disappearance of peaks from the allyl group and the regioisomer signaled full conversion into the corresponding tertiary amine PAES copolymer (TA-PAES). The <sup>1</sup>H NMR spectra for the A-PAES-XX series and TA-PAES-XX series with various TA-containing segment contents are shown in Figs. S2-3. Next, after conversion from the tertiary amine to the sulfobetaine, the peaks arising from the -CH<sub>2</sub>CH<sub>2</sub>N(CH<sub>3</sub>)<sub>2</sub> (signal l, m, n in Fig. 1c) shifted from 2.70, 3.08, and 2.67 ppm to 2.75, 3.11, and 2.72 ppm, respectively; also, new signals appeared at 3.71, 2.53, and 1.99 ppm, indicating the successful incorporation of sulfobetaine. Moreover, the integral of the peak from signal o, p, q agreed with the overall integral of the peak from signal l', m', n', confirming full conversion of the tertiary amine during the ring-opening reaction. The corresponding NMR spectra for the complete SB-PAES-XX series are shown in Fig. S4.

<sup>&</sup>lt;sup>b</sup> Determined by SEC LS detector measurement.

Y. Yang et al. Polymer 264 (2023) 125522

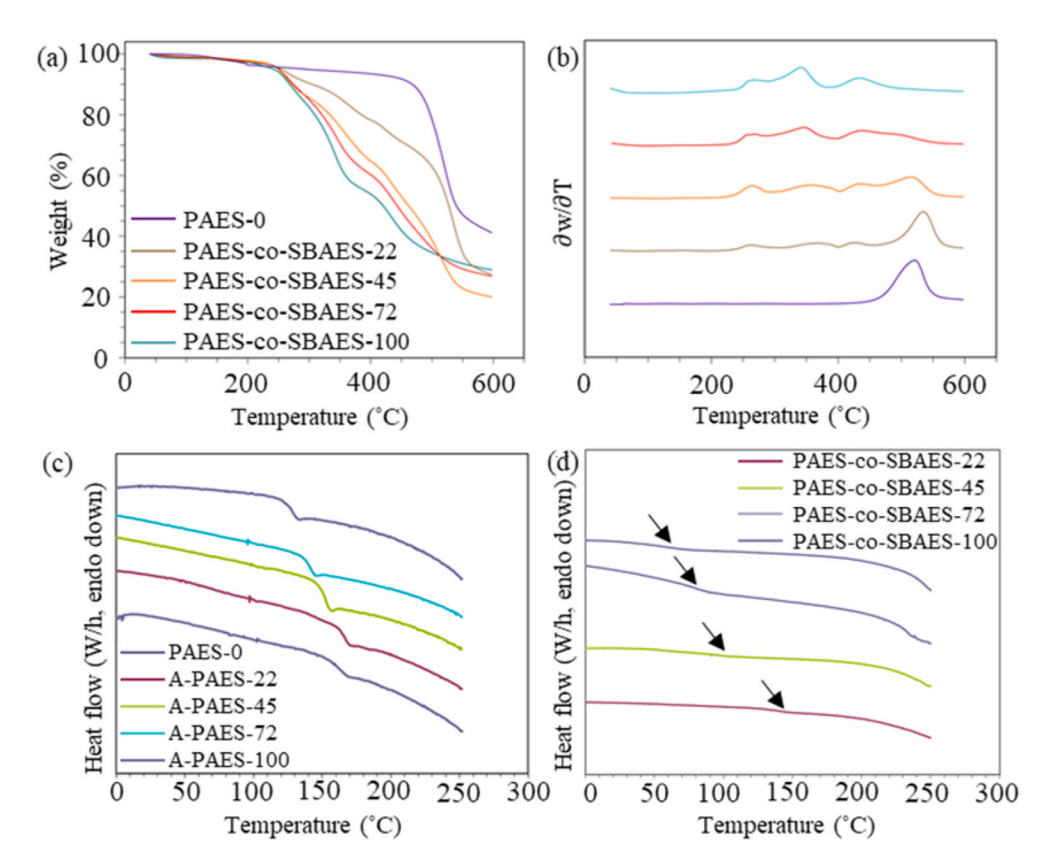


Fig. 2. (a) Thermogravimetric analysis traces and the corresponding (b) traces of differential weight with respect to temperature of zwitterionic poly(arylene ether sulfone) copolymers (PAES-co-SBAES-XX, XX = 22-100), as well as the uncharged PAES (PAES-0). Differential scanning calorimetry traces of (c) A-PAES-XX (XX = 0-100) copolymers, and (d) PAES-co-SBAES-XX (XX = 0-100) copolymers after annealing at 200 °C.

Introducing ionic functionality into polymeric materials has routinely reduced the thermal stability [27,28]. This could be induced by the thermal instability of the specific functional moieties, for instance, materials containing a quaternary ammonium are more susceptible to the Hofmann elimination around 250 °C. Therefore, the thermal stability of the SB-PAES-XX series was investigated using TGA. Fig. 2a and 2b show the sample weight as a function of temperature and the corresponding derivative of weight with respect to temperature for the series of zwitterionic PAES-co-SBAES copolymers. PAES-0 exhibited a one-step weight loss at a temperature of  $\sim 500$  °C, which was attributed to the degradation of the PAES backbone. In comparison with PAES-0, PAES-co-SBAES-XX showed multi-step weight losses. We analyze PAES-co-SBAES-100 as an example: above  $\sim$ 250  $^{\circ}$ C, the TGA scan shows several steps that we attribute to sequential breakdown of various parts of the pendant functional group followed by degradation of the polymer backbone at ~500 °C, which agrees with previous literature reports [14,29] and the decomposition behavior of PAES-0. Without spectrally analyzing the composition of the functional groups in the TGA outlet gas, it cannot be concluded what components of the copolymer degrade at what temperature. However, the magnitude of the step change in weight in the TGA trace, or the intensity of the peak in DTA trace, corresponding to the thermal degradation of chemical bonding in SBAES group was directly correlated with the ion-containing segment content in PAES-co-SBAES-XX. Thus, as shown in Fig. 2, the increase in the zwitterionic charge content from 0 mol% to 100 mol% results in an increase in the weight loss step attributed to the pendant side group and a corresponding decrease in the weight loss step of the polymer backbone. Thus, TGA confirmed the copolymer compositions and defined the thermal stability as ~250 °C due to the presence of the quaternary ammonium group in the copolymer.

Next, the copolymer thermal properties were analyzed using differential scanning calorimetry. These experiments shed light onto the glass

transition temperature (T<sub>g</sub>) and potentially onto the phase separation or formation of ionic aggregates (or lack thereof). Fig. 2c and d show the DSC heating traces recorded for A-PAES-XX (Fig. 2c) and PAES-co-SBAES-XX (Fig. 2d and Fig. S5), respectively. The Tos of the A-PAES copolymers progressively decreased with an increasing content of the DABA repeating unit. The "neat" PAES exhibited a  $T_g = 170\ ^{\circ}\text{C}$  and introducing 22 mol% of the DABA co-monomer caused an insignificant change in T<sub>g</sub>. However, further incorporation of allyl groups lowered the  $T_g$  of the copolymer all the way to 132 °C for A-PAES-100. Because the molecular weight of each copolymer is quite similar, we predict this trend is caused by a plasticization induced by the allyl group. The pendant allyl group introduces free volume and facilitates segmental motion at a lower temperature. Interestingly, after substituting the sulfobetaine side group, the copolymer  $T_g$ s decreased drastically relative to the corresponding A-PAES copolymer. Within the charged polymer series, the  $T_g$  decreased from 140  $^{\circ}\text{C}$  to 70  $^{\circ}\text{C}$  as the amount of SBAES increased from 22 mol% to 100 mol%, indicating the further plasticization effect by introducing the zwitterionic moieties. Additional features appeared around 240-250 °C (e.g., most notable in PAES-co-SBAES-100 and PAES-co-SBAES-72), but it is hard to draw a conclusion on whether this potential transition peak is attributed to the thermal degradation events or a second Tg caused by a microphase separated morphology due to the strong electrostatic interactions among the zwitterionic functionalities [30]. To probe this further, morphological analyses were performed using small-angle X-ray scattering and scanning transmission electron microscopy (Figs. S6-S8) which provided further insights into the absence of microphase aggregation. Thus, we predict the high temperature features in the DSC traces can be attributed to sample degradation.

The ability to tailor the hydrophilicity independently from the mechanical properties is considered the silver bullet for membrane materials, since it would increase water permeability without sacrificing

**Table 2**Mechanical properties, water uptake, and IEC of PAES-co-SBAES copolymers.

Membrane	Young's modulus (MPa)	Ultimate Stress (MPa)	Toughness (MPa)	Strain at break (%)	Water uptake (%)	$C_x^m \text{ (mol/L)}$	IEC (mmol/g)
PAES-co-SBAES-0	$4,937.1 \pm 359.5$	$91.8\pm31.2$	$3.56\pm2.70$	$3.9 \pm 1.6$	$7.5\pm1.3$	_	0
PAES-co-SBAES-22	_	_	-	-	$18.3\pm3.9$	$4.8\pm1.3$	0.84
PAES-co-SBAES-45	$66.8\pm10.7$	$9.1\pm4.4$	$0.10\pm0.06$	$3.0\pm0.4$	$34.3 \pm 8.8$	$\textbf{4.1} \pm \textbf{1.2}$	1.34
PAES-co-SBAES-72	$183.4\pm86.3$	$8.5 \pm 4.3$	$0.43\pm0.13$	$\textbf{5.7} \pm \textbf{1.8}$	$63.6 \pm 5.4$	$2.6\pm0.2$	1.67

mechanical strength. The mechanical properties of the zwitterionic PAES copolymers were determined using a uniaxial elongation tensile test and the results are summarized in Table 2. All samples were submerged in water for 24 h before the mechanical property tests in the aqueous environment, thus the water content of each sample during the mechanical property measurement is comparable with the water uptake reported in Table 2. The data are representative of multiple individual runs for each PAES-co-SBAES-XX (Table S1). Data could not be obtained for PAES-co-SBAES-22, as the films would dry and break when loading into the tensile testing apparatus. Overall, all tested membranes exhibited good mechanical properties in aqueous environments. The Young's modulus, ultimate stress, and toughness of the membranes decreased with the addition of SBAES content from 0% to 45%, which is presumably attributed to the plasticization effect by incorporating bulky pendant chains and agrees with the observation of a monotonic decrease in Tg with increasing SBAES content. However, the Young's modulus, toughness, and strain at break increased as the SBAES content increased from 45% to 72%. The ultimate stress for the 45% and 72% charge contents showed no statistically significant difference. To attempt to understand this trend, water uptake data for films of the PAES-co-SBAES copolymers with varying SBAES content were collected and are summarized in Table 2. It is worth noting that PAES-co-SBAES-100 is the only sample soluble in water among the PAES-co-SBAES series, thus it is not possible to measure the mechanical properties in an aqueous environment or perform the water uptake experiment. The results indicate a substantial increase in absorbed water with an increase in the SBAES content, which is rationalized by the hydrophilic nature of the zwitterionic groups. The water uptake data is used to calculate the fixed charge concentration of the polymers (Table 2), which decreases 14.6% as the IEC increases from 0.84 mmol/g to 1.34 mmol/g (PAES-co-SBAES-22 to PAES-co-SBAES-45, i.e.,  $\sim$ 60% increase in IEC) and decreases 36.6% as the IEC increases from 1.34 mmol/g to 1.67 mmol/g (PAES-co-SBAES-45 to PAES-co-SBAES-72, i.e., ~27% increase in IEC). These data provide interesting insights into the material performance, and we analyze each change in composition separately. When the charge content increases from 22% to 45% the material exhibits an increase in IEC and water sorption that are similar in magnitude (~60% and ~87%, respectively). When the charge content increases from 45% to 72%, the increase in IEC is  $\sim$ 27% but the water uptake is similar in magnitude to the previous jump, ~85%. This results in a similar fixed charge concentration (in mol charge/L water sorbed) for the 22% and 45% charge contents, but a much smaller fixed charge concentration at 72% SBAES. Therefore, the water uptake and uniaxial tensile experiments correlate to one another. The neutral polymer (PAES- 0) displays unique behavior: good mechanical properties and a low water uptake. However, the zwitterion copolymers have a different trend. The PAES-co-SBAES-22 copolymer could not form a stable film when hydrated, the samples broke almost instantaneously. Then, the strain at break, Young's modulus, and toughness all increase when the charge content goes from 45% to 72% and the fixed charge concentration decreases by 37%. Thus, we predict that the zwitterions form intermolecular ion bridges that serve as physical crosslinks to improve the mechanical performance from 22% to 72% charge content. As noted above, the steady increase in water uptake decreases the fixed charge concentration; but, in spite of this, the mechanical properties improve because of the physical crosslinks.

#### 4. Conclusions

In this work, a series of zwitterionic PAES copolymers with controllable sulfobetaine charge content (0-100%) and high molecular weight (M<sub>w</sub> ~ 65 kDa) was successfully synthesized by a polycondensation reaction and post-polymerization functionalization reactions. The thermal degradation temperature of all the zwitterionic PAESs studied is above 250  $^{\circ}\text{C}$ . The STEM and X-ray scattering data independently, and corroboratively, confirmed the absence of the microphase separation, which supported the observation of a single  $T_g$  in DSC for all zwitterionic PAESs. Thus, the ion aggregation expected to be present was restricted by the rigidity and the relatively high polarity of the high T<sub>g</sub> PAES backbone. In addition, the T<sub>g</sub> and mechanical strength (Young's modulus) decreased with the incorporation of the charge group, which suggests a plasticization effect by the zwitterion. Furthermore, the hydrophilicity of the studied film was evaluated by water uptake measurements, where the water uptake of the zwitterionic PAESs increased up to 64 wt% for the PAES-co-SBAES-72 sample. The freestanding film in the wet state exhibited an average Young's modulus of up to 183.4  $\pm$  86.3 MPa. This investigation provides insight into the design of charge-containing thermoplastics that are potentially useful for coating and membrane purification applications, including the connection between charge density, thermomechanical performance, and morphology.

#### CRediT authorship contribution statement

Yi Yang: Conceptualization, Methodology, Validation, Formal analysis, Investigation, Writing – original draft, Writing – review & editing, Visualization. Hoda Shokrollahzadeh Behbahani: Methodology, Validation, Formal analysis, Investigation, Writing – review & editing, Visualization. Brian F. Morgan: Methodology, Validation, Formal analysis, Investigation, Writing – review & editing, Visualization. Frederick L. Beyer: Methodology, Validation, Formal analysis, Investigation, Writing – review & editing, Visualization. Alexis Hocken: Validation, Formal analysis, Investigation, Writing – review & editing. Matthew D. Green: Conceptualization, Methodology, Validation, Formal analysis, Investigation, Resources, Writing – review & editing, Visualization, Supervision, Project administration, Funding acquisition.

#### **Declaration of competing interest**

The authors declare that they have no known competing financial interests or personal relationships that could have appeared to influence the work reported in this paper.

#### Data availability

Data will be made available on request.

#### Acknowledgements

The authors gratefully acknowledge funding from the following sponsors: NASA ECF 80NSSC18K1508, NSF CBET 1836719 and ARO W911NF-15-1-0353. The information, data, or work presented herein was funded in part by the Advanced Research Projects Agency-Energy (ARPA-E, U.S. Department of Energy, under Award Number DE-

AR0001103. The views and opinions of authors expressed herein do not necessarily state or reflect those of the United States Government or any agency thereof.

#### Appendix A. Supplementary data

Supplementary data to this article can be found online at https://doi.org/10.1016/j.polymer.2022.125522.

#### References

- J. Chang, A.M. Lenhoff, S.I. Sandler, Solvation free energy of amino acids and sidechain analogues, J. Phys. Chem. B 111 (2007) 2098–2106, https://doi.org/ 10.1021/in0620163
- [2] C. Liu, J. Lee, J. Ma, M. Elimelech, Antifouling thin-film composite membranes by controlled architecture of zwitterionic polymer brush layer, Environ. Sci. Technol. (2017), https://doi.org/10.1021/acs.est.6b05992.
- [3] Y.F. Zhao, P. Bin Zhang, J. Sun, C.J. Liu, L.P. Zhu, Y.Y. Xu, Electrolyte-responsive polyethersulfone membranes with zwitterionic polyethersulfone-based copolymers as additive, J. Membr. Sci. (2016), https://doi.org/10.1016/j. memsci.2016.03.006.
- [4] R. Ma, Y.L. Ji, X.D. Weng, Q.F. An, C.J. Gao, High-flux and fouling-resistant reverse osmosis membrane prepared with incorporating zwitterionic amine monomers via interfacial polymerization, Desalination (2016), https://doi.org/10.1016/j. desal.2015.11.023.
- [5] D. Faulón Marruecos, D.K. Schwartz, J.L. Kaar, Impact of surface interactions on protein conformation, Curr. Opin. Colloid Interface Sci. (2018), https://doi.org/ 10.1016/j.cocis.2018.08.002.
- [6] P. Bengani-Lutz, E. Converse, P. Cebe, A. Asatekin, Self-assembling zwitterionic copolymers as membrane selective layers with excellent fouling resistance: effect of zwitterion chemistry, ACS Appl. Mater. Interfaces (2017), https://doi.org/ 10.1021/acsami.7b04884.
- [7] J. Parvole, P. Jannasch, Polysulfones grafted with poly(vinylphosphonic acid) for highly proton conducting fuel cell membranes in the hydrated and nominally dry state, Macromolecules (2008), https://doi.org/10.1021/ma800042m.
- [8] P. Sae-Ung, K.W. Kolewe, Y. Bai, E.W. Rice, J.D. Schiffman, T. Emrick, V.P. Hoven, Antifouling stripes prepared from clickable zwitterionic copolymers, Langmuir (2017), https://doi.org/10.1021/acs.langmuir.7b01431.
- [9] Q. Li, J. Imbrogno, G. Belfort, X.L. Wang, Making polymeric membranes antifouling via "grafting from" polymerization of zwitterions, J. Appl. Polym. Sci. (2015), https://doi.org/10.1002/app.41781.
- [10] W.W. Yue, H.J. Li, T. Xiang, H. Qin, S.D. Sun, C.S. Zhao, Grafting of zwitterion from polysulfone membrane via surface-initiated ATRP with enhanced antifouling property and biocompatibility, J. Membr. Sci. (2013), https://doi.org/10.1016/j. memsci.2013.06.029.
- [11] Y.F. Yang, Y. Li, Q.L. Li, L.S. Wan, Z.K. Xu, Surface hydrophilization of microporous polypropylene membrane by grafting zwitterionic polymer for anti-biofouling, J. Membr. Sci. (2010), https://doi.org/10.1016/j.memsci.2010.06.048.
- [12] J.M. Dennis, G.B. Fahs, N.G. Moon, R.J. Mondschein, R.B. Moore, G.L. Wilkes, T. E. Long, Synthesis of polysulfone-containing poly(butylene terephthalate) segmented block copolymers: influence of segment length on thermomechanical performance, Macromolecules (2017), https://doi.org/10.1021/acs.macromol.7b00557.

- [13] J.M. Dennis, G.B. Fahs, R.B. Moore, S.R. Turner, T.E. Long, Synthesis and characterization of polysulfone-containing poly(butylene terephthalate) segmented block copolymers, Macromolecules (2014), https://doi.org/10.1021/ pa501903b
- [14] Q. Zhang, S. Zhang, S. Li, Synthesis and characterization of novel cardo poly(aryl ether sulfone) bearing zwitterionic side groups for proton exchange membranes, Int. J. Hydrogen Energy (2011), https://doi.org/10.1016/j.ijhydene.2011.01.144.
- [15] Q. Zhang, S. Zhang, L. Dai, X. Chen, Novel zwitterionic poly(arylene ether sulfone)s as antifouling membrane material, J. Membr. Sci. 349 (2010) 217–224, https://doi.org/10.1016/j.memsci.2009.11.048.
- [16] J. Kamcev, D.R. Paul, B.D. Freeman, Effect of fixed charge group concentration on equilibrium ion sorption in ion exchange membranes, J. Mater. Chem. A. 5 (2017) 4638–4650, https://doi.org/10.1039/c6ta07954g.
- [17] S.R. Choudhury, O. Lane, D. Kazerooni, G.S. Narang, E.S. Jang, B.D. Freeman, J. J. Lesko, J.S. Riffle, Synthesis and characterization of post-sulfonated poly(arylene ether sulfone) membranes for potential applications in water desalination, Polymer (Guildf) 177 (2019) 250–261, https://doi.org/10.1016/j.polymer.2019.05.075.
- [18] J. Kamcev, C.M. Doherty, K.P. Lopez, A.J. Hill, D.R. Paul, B.D. Freeman, Effect of fixed charge group concentration on salt permeability and diffusion coefficients in ion exchange membranes, J. Membr. Sci. (2018), https://doi.org/10.1016/j. memsci.2018.08.053.
- [19] A. Daryaei, E.S. Jang, S. Roy Choudhury, D. Kazerooni, J.J. Lesko, B.D. Freeman, J. S. Riffle, J.E. McGrath, Structure-property relationships of crosslinked disulfonated poly(arylene ether sulfone) membranes for desalination of water, Polymer (Guildf) 132 (2017) 286–293, https://doi.org/10.1016/j.polymer.2017.10.056.
- [20] J. Ilavsky, Nika: software for two-dimensional data reduction, J. Appl. Crystallogr. 45 (2012) 324–328, https://doi.org/10.1107/S0021889812004037.
- [21] J. Ilavsky, P.R. Jemian, Irena: tool suite for modeling and analysis of small-angle scattering, J. Appl. Crystallogr. 42 (2009) 347–353, https://doi.org/10.1107/ S0021889809002222.
- [22] J.F. Bunnett, R.E. Zahler, Aromatic nucleophilic substitution reactions, Chem. Rev. (1951), https://doi.org/10.1021/cr60153a002.
- [23] S.D. Ross, R.C. Petersen, Nucleophilic displacement reactions in aromatic systems. II. Catalysis of the reaction of 2,4-dinitrochlorobenzene and n-butylamine by triethylamine in chloroform, J. Am. Chem. Soc. 80 (1958) 2447–2449, https://doi.org/10.1021/ja01543a025.
- [24] B.E. Jennings, M.E.B. Jones, J.B. Rose, Synthesis of poly(arylene sulfones) and poly (arylene ketones) by reactions involving substitution at aromatic nuclei, J. Polym. Sci. Part C Polym. Symp. (2007), https://doi.org/10.1002/polc.5070160212.
- [25] Y. Yang, C.L. Muhich, M.D. Green, Kinetics and mechanisms of polycondensation reactions between aryl halides and bisphenol A, Polym. Chem. 11 (2020) 5078–5087. https://doi.org/10.1039/d0pv00740d.
- [26] J.J. Gajewski, C3H4-C3H6, Hydrocarb. Therm. Isomerizations. (2004) 19–32, https://doi.org/10.1016/b978-012273351-2/50005-1.
- [27] D.L. Feldheim, D.R. Lawson, C.R. Martin, Influence of the sulfonate countercation on the thermal stability of nafion perfluorosulfonate membranes, J. Polym. Sci., Part B: Polym. Phys. (1993), https://doi.org/10.1002/polb.1993.090310805.
- [28] B. Grassl, B. Meurer, M. Scheer, J.C. Galin, Segmented poly(tetramethylene oxide) zwitterionomers and their homologous ionenes. 2. Phase separation through DSC and solid state 1H-NMR spectroscopy, Macromolecules (1997), https://doi.org/ 10.1021/ma960643s
- [29] J. Liu, Y. Ma, T. Xu, G. Shao, Preparation of zwitterionic hybrid polymer and its application for the removal of heavy metal ions from water, J. Hazard Mater. (2010), https://doi.org/10.1016/j.jhazmat.2010.02.041.
- [30] E. Marwanta, T. Mizumo, H. Ohno, Improved ionic conductivity of nitrile rubber/ Li(CF3SO2)2N composites by adding imidazolium-type zwitterion, Solid State Ionics (2007), https://doi.org/10.1016/j.ssi.2006.12.022.